Non-Hermitian Physics in Mesoscopic Electron Transport Through Coupled Quantum Dots

Yiyang Li[1], Jincheng Lu[2,3*], Chen Wang[4*], and Jian-Hua Jiang[1,5,6,7*]

[1]*School of Physical Science and Technology & Collaborative Innovation Center of Suzhou Nano Science and Technology, Soochow University, Suzhou 215006, China*
[2]*Key Laboratory of Intelligent Optoelectronic Devices and Chips of Jiangsu Higher Education Institutions, School of Physical Science and Technology, Suzhou University of Science and Technology, Suzhou 215009, China*
[3]*Advanced Technology Research Institute of Taihu Photon Center, School of Physical Science and Technology, Suzhou University of Science and Technology, Suzhou 215009, China*
[4]*Department of Physics, Zhejiang Normal University, Jinhua 321004, China*
[5]*School of Biomedical Engineering, Division of Life Sciences and Medicine, University of Science and Technology of China, Hefei 230026, China*
[6]*Suzhou Institute for Advanced Research, University of Science and Technology of China, Suzhou 215123, China*
[7]*School of Physical Sciences, University of Science and Technology of China, Hefei 230026, China*

(Received 13 February 2025; accepted manuscript online 24 March 2025)

We investigate electron mesoscopic transport in a three-terminal setup with coupled quantum dots and a magnetic flux. By mapping the original transport problem into a non-Hermitian Hamiltonian form, we study the interplay between the coherent couplings between quantum dots, the magnetic flux, and the dissipation due to the tunnel coupling with the reservoirs. We explore the emergence of exceptional points (EPs) and their impact on the charge transport, particularly, the chiral currents. We further analyze the effective Hamiltonian to identify conditions under which EPs arise and the role of parity-time ($\mathcal{PT}$) symmetry. These EPs are shown to govern the spectral singularities and dramatically affect the dynamical behavior of chiral currents. We also show that the transmission function in the Landauer formula can be expressed in simpler forms using the non-Hermitian eigenstates. By examining the transmission function, we establish the relationship between $\mathcal{PT}$ symmetry, EPs, and peaks in the transmission spectrum. Our findings could provide a deeper understanding of non-Hermitian quantum effects in electron tranpsort phenomena, offering valuable insights for the design of tunable non-Hermitian chiral quantum devices with engineered transport properties.

DOI: 10.1088/0256-307X/42/4/047303 CSTR: 32039.14.0256-307X.42.4.047303

Introduction. The conservation laws of energy and matter play fundamental roles in constraining physical evolution and reality. Non-Hermiticity,[1–3] emerging from the connection of physical systems with surrounding environments, generally breaks conservation laws, offering powerful non-Hermitian platforms in metamaterials,[4–6] photonics,[7–10] and acoustics.[11–13] One crucial milestone in non-Hermitian quantum mechanics was the remarkable discovery of the singular spectra, i.e., exceptional points (EPs),[14] where eigenvalues and eigenvectors simultaneously coalesce. The eigenvalues of non-Hermitian systems remain real when preserving $\mathcal{PT}$ symmetry, whereas complex eigenvalues arise when $\mathcal{PT}$ symmetry is broken.[15] Such singular feature of EPs has led to a range of exciting physical applications, including quantum-enhanced sensors,[16–19] efficiency-enhanced quantum heat engines,[20,21] the non-Hermitian skin effect,[22–26] the non-Hermitian Sagnac effect,[27,28] and non-Hermitian topology.[29–31] Higher-order EPs have also been discovered, which further enhance sensitivity compared to the standard second-order EP.[16,32,33] Furthermore, the EP can also be understood within the framework of Liouvillian algebra,[34–36] giving rise to the concept of Liouvillian EPs, which differ from the non-Hermitian Hamiltonian counterpart.

In the realm of mesoscopic physics, quantum transport plays a central role in understanding the flow of charge, spin, and energy in nanoscale systems. Mesoscopic transport, characterized by phase coherence and quantum interference effects, provides a rich platform for exploring non-Hermitian phenomena, particularly in understanding the interplay between phase coherence, chirality, and dissipation. The study of mesoscopic transport in non-Hermitian formalism is not only fundamental for deeper understanding of quantum coherence and dissipation but also crucial for designing advanced quantum devices with engineered transport properties.

This work investigates a non-Hermitian version of a coupled triple-quantum-dot system driven by a chiral field. Chirality at the nanoscale has garnered signifi-

*Corresponding author. Email: jinchenglu@usts.edu.cn; wangchen@zjnu.cn; jhjiang3@ustc.edu.cn
© 2025 Chinese Physical Society and IOP Publishing Ltd. All rights, including for text and data mining, AI training, and similar technologies, are reserved.

cant attention, offering promising platforms for quantum optics,[37,38] strongly correlated many-body systems,[39,40] photon blockade,[41] and quantum thermodynamics.[42,43] When combined with non-Hermiticity, chirality plays a pivotal role in phenomena such as heat transport,[44] squeezed phononics,[45] $\mathcal{PT}$ transmission,[46] and chiral symmetry breaking.[38,47] Therefore, it is particularly intriguing to investigate EP and chiral transport in non-Hermitian coupled quantum dot rings.

In this Letter, what sets our work apart is the unique combination of non-Hermiticity, chirality, and mesoscopic transport in a triple-quantum-dot system. Our system allows for the precise control of chiral currents and the exploration of EPs in the context of mesoscopic quantum transport setup. By analyzing the effective non-Hermitian Hamiltonian, we uncover the emergence of second- and third-order EPs in electron's Hilbert space, rather than the more classical mode space as studied in photonic and other bosonic systems. These EPs are shown to govern the spectral singularities and dramatically affect the dynamical behavior of chiral currents. We show necessary conditions to realize EPs and examine their impact on the system's transient chiral currents both with and without $\mathcal{PT}$ symmetry. We also introduce the transmission function in non-Hermitian framework. The transmission function reveals a strong correlation between EPs and $\mathcal{PT}$ symmetry. The interplay between the chiral field, tunneling interactions, and incoherent exchange processes gives rise to the emergence of exceptional points and chiral transport. Our findings reveal the intricate non-Hermitian physics underlying the triple-quantum-dot system, providing valuable insights for the design of non-Hermitian chiral quantum devices with tunable transport properties.

$\mathcal{PT}$ symmetry in a non-Hermitian triple-quantum-dot system. The non-Hermitian quantum model in Fig. 1 consists of three coupled quantum dots, collectively driven by a coherent chiral field and subjected to incoherent gain and loss processes. The effective Hamiltonian is expressed as

$$\hat{H}_{\rm eff} = \hat{H}_{\rm QD} + {\rm i}\gamma_1 \hat{c}_1^\dagger \hat{c}_1 - {\rm i}\gamma_2 \hat{c}_2^\dagger \hat{c}_2. \tag{1}$$

The chiral triple quantum dots are described by the Hamiltonian[50]

$$\begin{aligned}\hat{H}_{\rm QD} = {} & \varepsilon_1 \hat{c}_1^\dagger \hat{c}_1 + \varepsilon_2 \hat{c}_2^\dagger \hat{c}_2 + \varepsilon_3 \hat{c}_3^\dagger \hat{c}_3 \\ & + \delta {\rm e}^{{\rm i}\phi} \left(\hat{c}_1^\dagger \hat{c}_2 + \hat{c}_2^\dagger \hat{c}_3 + \hat{c}_3^\dagger \hat{c}_1 \right) + {\rm H.c.},\end{aligned} \tag{2}$$

where $\hat{c}_i^\dagger$ ($\hat{c}_i$) represents the creation (annihilation) operator for an electron in the i-th quantum dot, with an energy level ε_i. We set $\varepsilon = \varepsilon_i$ ($i = 1, 2, 3$). The parameter δ denotes the nearest-neighbor hopping strength, while ϕ represents the phase of the chiral field. Hence, the total phase around the electron ring is 3ϕ. γ_1 denotes the incoherent gain strength, which may be operated via the incoherent optical pump in the first dot. γ_2 means the incoherent loss strength of the second dot. While the dissipation of the third dot is assumed to be negligible. We set the identical relation of gain and loss strengths, i.e., $\gamma_1 = \gamma_2 = \gamma$. The proposed system can be experimentally realized using semiconductor quantum dots embedded in nanophotonic circuits or superconducting quantum circuits,[48] where chiral coupling[37] and magnetic flux[49] can be engineered via spin-momentum locking or external magnetic fields.

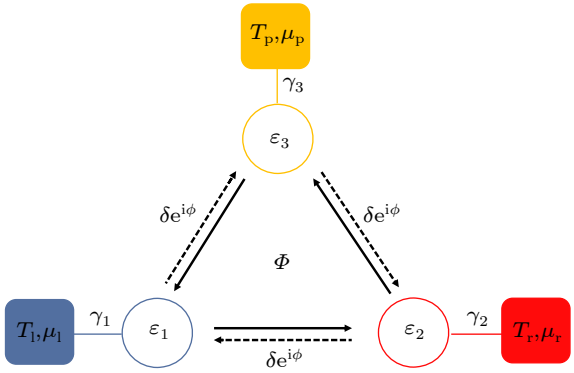

Fig. 1. Schematic diagram of a triple-QD thermoelectric device under a piercing magnetic flux ϕ. Three quantum dots with a single energy level ε_i ($i = 1, 2, 3$) are connected in series to three fermionic reservoirs i ($i = {\rm l}, {\rm r}, {\rm p}$). The electric reservoirs have temperatures denoted as T_i, while their respective chemical potentials are represented as μ_i. δ is the tunneling between the QDs. γ_1 and γ_2 represent the gain and loss rates, respectively, describing the coupling between the quantum dots and their external environments.

Exceptional point may be reflected via the system's dynamical properties and are closely tied to the interaction between the chiral field and gain and loss. To locate the exceptional points, we first analyze the characteristic equation of the Hamiltonian $\hat{H}_{\rm eff}$, defined by $\det[(E+\varepsilon)\hat{I} - \hat{H}_{\rm eff}] = 0$. Based on the seminal Cardano–Tartaglia method, we have three real eigenvalues under the criterion

$$\Delta = \{[\delta^3 \cos(3\phi)]^2 + (\gamma^2/3 - \delta^2)^3\} \leq 0, \tag{3}$$

which corresponds to the $\mathcal{PT}$ symmetry case, whereas one real eigenvalue and two conjugate complexes appear for $\Delta > 0$, demonstrating $\mathcal{PT}$ symmetry broken. Thus the sign of Δ is crucial to determine the $\mathcal{PT}$ behavior of the non-Hermitian system, from the eigenvalues perspective. Moreover, it is easy to find that Δ is positive once $\phi = 0$ and $\gamma \neq 0$, implying the absence of EP. We also analytically obtain one full degenerate solution ($E = 0$) by setting $\Delta = 0$, i.e., $\cos 3\phi = 0$ and $\gamma = \sqrt{3}\delta$, which denotes the critical positions of third-order exceptional point (EP3). This demonstrates the absence of EP if we tune up $\gamma > \sqrt{3}\delta$ regardless of ϕ.

We investigate the influence of the chiral phase ϕ on the eigenspectrum of the effective Hamiltonian (1). Figures 2(ai), 2(bi), and 2(ci) illustrate the real parts of the eigenvalues for gain-loss parameters $\gamma = \delta$, $\gamma = \sqrt{3}\delta$, and $\gamma = 2\delta$, respectively, whereas (aii), (bii), and (cii) depict the corresponding imaginary parts. In Figs. 2(ai) and 2(aii) with $\gamma = \delta$, the spectrum shows mirror symmetry at $3\phi/2\pi = 0.5$. Second-order exceptional points (EP2s) are observed by tuning ϕ, e.g., at $3\phi/2\pi \approx 0.3$. The successive

regions of $\mathcal{PT}$ symmetry and symmetry breaking are classified. The chiral positions can be determined from Eq. (3) as

$$\phi^{\rm c}_{n,\pm} = \frac{(n\mp 1)\pi}{3} \pm \frac{1}{3}\arccos\left[(1-\gamma^2/3\delta^2)^{3/2}\right], \tag{4}$$

with $n = 1, 2$. Hence, we are able to generally obtain four critical transition chiral phases.

As γ increases to $\sqrt{3}\delta$, these EP2s merge into two EP3s[32] at $\phi^{\rm c} = \pi/6$ and $\pi/2$, as evident in Figs. 2(bi) and 2(bii). The fusion of EP2s into higher-order EP3s represents a critical transition by tuning ϕ. Such higher-order EP behavior may improve the sensitivity of the non-Hermitian system.[16] When γ further increases beyond $\gamma/\delta = \sqrt{3}$, e.g., $\gamma = 2\delta$ in Figs. 2(ci) and 2(cii), the real parts of the eigenvalues retain their merging positions at $3\phi/2\pi = 0.25$ and $3\phi/2\pi = 0.75$, whereas the imaginary parts no longer exhibit degeneracy. Hence, we conclude that the non-Hermitian system always keeps $\mathcal{PT}$ symmetry breaking. To better show the influences of δ and ϕ on exceptional points more, we also draw a bird view in Fig. 3, where the EP boundary can be identified (white circles) from both real and imaginary parts.

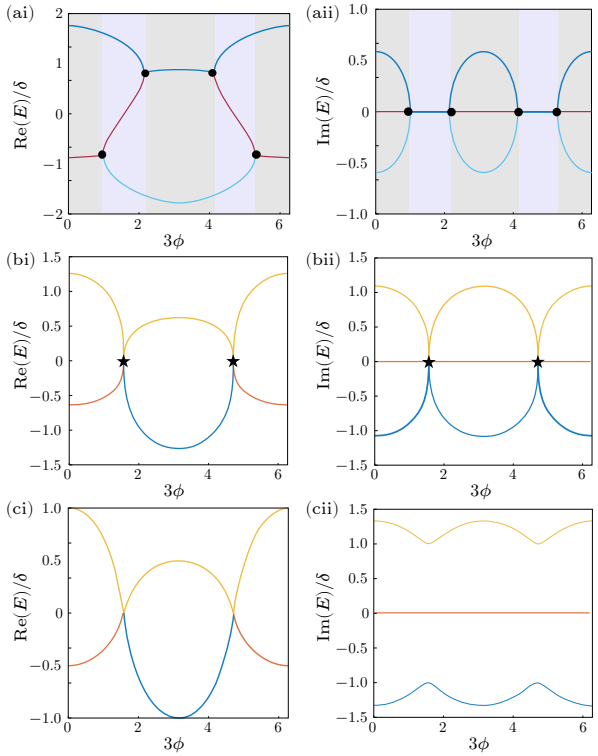

Fig. 2. Real and imaginary parts of the eigenvalues of the effective Hamiltonian $H_{\rm eff}$ as functions of the phase ϕ of the chiral field, shown for three regimes: (a) $\gamma = \delta$, (b) $\gamma = \sqrt{3}\delta$, and (c) $\gamma = 2\delta$, with $\gamma_1 = \gamma_2 = \gamma$. The real parts represent the energy spectrum of the system, while the imaginary parts reflect the gain and loss dynamics induced by the coupling to the reservoirs. The interplay between the chiral field and non-Hermitian effects leads to characteristic behaviors by varying ϕ, such as eigenvalue crossings and possible exceptional points. In panels (ai) and (aii), the black circles represent EP3, while the black pentagons in panels (bi) and (bii) denote EP2. The other parameters are given by $\varepsilon_1 = \varepsilon_2 = \varepsilon_3 = 0$.

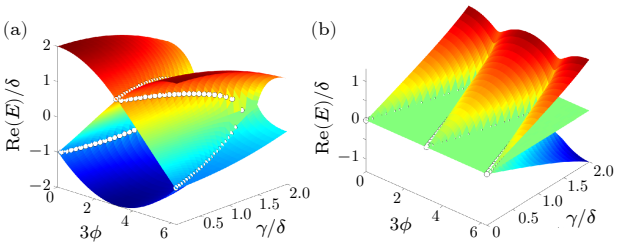

Fig. 3. Real part Re(E) and imaginary part Im(E) of the eigenvalue of the effective Hamiltonian $H_{\rm eff}$ as functions of the phase ϕ of the chiral field and the gain-loss strength γ. The white circles are EP positions from Eq. (4). The other parameters are given by $\varepsilon_1 = \varepsilon_2 = \varepsilon_3 = 0$.

The non-Hermitian nature of the triple quantum dot system may be signified by the dynamics of chiral currents. Based on the continuity equation of populations (see SI), the current between two dots m and n (m, $n = 1, 2, 3$) is expressed as $I_{mn} = -{\rm i}\delta {\rm e}^{{\rm i}\phi}\langle \hat{c}^\dagger_m \hat{c}_n\rangle + {\rm H.c.}$. Consequently, the total chiral current through the system is defined as the sum of the components between adjacent quantum dots, given by

$$I = I_{12} + I_{23} + I_{31}. \tag{5}$$

The total current I captures the cumulative flow of energy across the system. This non-reciprocal current is a hallmark of chiral transport in non-Hermitian systems and may manifest the role of exceptional points in modulating transport properties. The chiral current described here can be experimentally realized in semiconductor quantum dot arrays or superconducting circuits, where directional electron flow and phase-controlled tunneling have been demonstrated.[37]

Figure 4 examines the influence of the chiral phase on the dynamics of the chiral current in the context of $\mathcal{PT}$ symmetry. In panel Fig. 4(a) with $\gamma = \delta$, the chiral current is able to exhibit long-time oscillations. In the $\mathcal{PT}$ symmetry-preserving regions, e.g., $\phi = \pi/6$ and $\phi = \pi/2$, large-amplitude oscillations are observed. These oscillations correspond to the presence of three real eigenvalues of $H_{\rm eff}$. While the $\mathcal{PT}$ symmetry-breaking regions, e.g., $\phi = 0$ and $\pi/4$, two complex eigenvalues are obtained, which result in the rapid stabilization of the chiral currents. It should be noted that the dynamic switch from non-decay oscillations of the chiral current within the $\mathcal{PT}$ symmetry region to fast stabilization with $\mathcal{PT}$ symmetry breaking signifies EP. Therefore, the EPs serve as a dividing line between areas of long-time oscillatory and non-oscillatory behaviors.

Figure 4(b) with $\gamma = \sqrt{3}\delta$ exhibits a distinctly different behavior of the chiral current. The system resides predominantly in the $\mathcal{PT}$ symmetry-breaking regime. While for $\mathcal{PT}$ symmetry-preserving positions, the eigenvalues of $H_{\rm eff}$ are zero. As a result, the current grows rapidly before stabilizing, without noticeable oscillations. Furthermore, the system with $\gamma = 2\delta$ remains in the $\mathcal{PT}$ symmetry-breaking regime for all values of ϕ in Fig. 4(c). The evolution of chiral current mirrors that of Fig. 4(b), but with a shorter timescale to stabilization. Therefore, the signature of EPs

can indeed be detected via the dynamic behaviors of the chiral current.

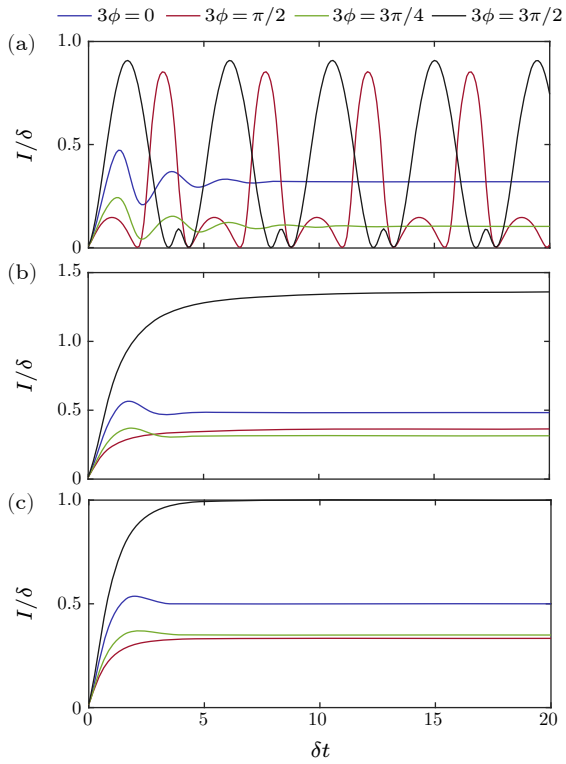

Fig. 4. Time evolution of the normalized chiral currents I/δ for different values of the chiral phase ϕ, shown for three regimes: (a) $\gamma = \delta$, (b) $\gamma = \sqrt{3}\delta$, and (c) $\gamma = 2\delta$. In (a), $3\phi = 0$ and $3\pi/4$ correspond to $\mathcal{PT}$ symmetry-breaking phases, while $3\phi = \pi/2$ and $3\pi/2$ correspond to $\mathcal{PT}$-symmetric phases, with EP2s separating these regions. In (b), $3\phi = \pi/2$ and $3\pi/2$ correspond to EP3s, while other values of ϕ result in $\mathcal{PT}$ symmetry breaking. In (c), all cases correspond to $\mathcal{PT}$ symmetry breaking. The other parameters are given by $\varepsilon_1 = \varepsilon_2 = \varepsilon_3 = 0$. The initial state is set as $c_1^\dagger|0\rangle$.

We note that the exceptional points in this study are obtained by exploring the eigenvalues of the real quantum Hamiltonian of the non-Hermitian coupled quantum dots in the Hilbert electron states. Though the analogous EPs can also be observed in oscillator trimers,[38] the effective Hamiltonian is alternatively constructed by analyzing the evolution matrix of boson modes, rather than in the Hilbert space.

Non-Hermitian Transmission Function. The transmission effect is central to quantum transport in mesoscopic systems, e.g., charge and energy transfer across quantum dots.[51] Landauer's formula established the relationship between conductance and transmission probability,[52] forming the basis for studying phenomena like tunneling and quantum interference.[53] In non-Hermitian systems, transmission becomes more complex by including effects like exceptional points and chiral transmission,[46] which should be crucial for designing new non-Hermitian devices.

Generally, the transmission probability function $\mathcal{T}_{ij}(\omega)$ from terminal j to terminal i is described as[53]

$$\mathcal{T}_{ij}(\omega) = \mathrm{Tr}[\hat{\Gamma}_i \hat{G}(\omega)\hat{\Gamma}_j \hat{G}^\dagger(\omega)], \tag{6}$$

where the retarded system Green function operator denotes $\hat{G}(\omega) \equiv [\omega\hat{I} - \hat{H}_\mathrm{S} - \mathrm{i}\hat{\Gamma}/2]^{-1}$, $\hat{H}_\mathrm{S}$ means the quantum system, e.g., quantum dots in this work, the damping matrix $\hat{\Gamma}$ is expressed as $\hat{\Gamma} = \sum_j \hat{\Gamma}_j$, with the incoherent hopping operator $\hat{\Gamma}_j = \gamma_j|j\rangle\langle j|$, local occupation state $|j\rangle = \hat{c}_j^\dagger|0\rangle$, and γ_j the dissipation strength in the wide-band limit. In previous works, the researchers mainly focus on the possible solution of $\hat{H}_\mathrm{S}$ to solve the transmission function.

We introduce the effective non-Hermitian Hamiltonian as

$$\hat{H}_\mathrm{eff} = \omega\hat{I} - \hat{G}^{-1}(\omega), \tag{7}$$

which can be equivalently expressed as $\hat{H}_\mathrm{eff} = \hat{H}_\mathrm{S} + \mathrm{i}\hat{\Gamma}/2$. Thus the retarded Green function can be reexpressed from the non-Hermitian picture, which is distinct from the traditional Hermitian counterpart. This understanding was adopted in several interesting non-Hermitian studies.[54,55] This effective Hamiltonian represents a critical modification of the traditional Hermitian counterpart by incorporating the non-Hermitian nature of the system-reservoir interactions, which may result in EP. This approach allows us to capture the essential physics of non-Hermitian quantum systems. Hence, it may be an essential utility for efficiently manipulating non-Hermitian quantum systems in non-equilibrium transport devices.

Intriguingly, the imaginary components of $\hat{H}_\mathrm{eff}$ dramatically affect the broadening and shift of peaks in the transmission function $\mathcal{T}_{ij}(E)$. These non-Hermitian terms may break reciprocity and give rise to unidirectional behavior in the chiral currents. Furthermore, the system may also exhibit exceptional points (EPs), where eigenvalues and eigenvectors of $\hat{H}_\mathrm{eff}$ coalesce, producing unique transport signatures such as abrupt enhancement of $\mathcal{T}_{ij}(\omega)$.

If one expresses the Green's function operator in terms of the eigenstates $|\psi_n\rangle$ and $|\phi_n\rangle$ of the effective Hamiltonian $\hat{H}_\mathrm{eff}$ and $\hat{H}_\mathrm{eff}^\dagger$, i.e., $\hat{H}_\mathrm{eff}|\psi_n\rangle = E_{n,\psi}|\psi_n\rangle$ and $\hat{H}_\mathrm{eff}^\dagger|\phi_n\rangle = E_{n,\phi}|\phi_n\rangle$ with $E_{n,\phi} = E_{n,\psi}^*$, the operator is specified as

$$\hat{G}(\omega) = \sum_n \frac{|\psi_n\rangle\langle\phi_n|}{(\omega - E_{n,\psi})\langle\phi_n|\psi_n\rangle}, \tag{8}$$

by considering the identity operator $\hat{I} = \sum_n |\psi_n\rangle\langle\phi_n|/\langle\phi_n|\psi_n\rangle = \sum_n |\phi_n\rangle\langle\psi_n|/\langle\psi_n|\phi_n\rangle$. We note that it is rather important to yield the explicit expression of the transmission function in the non-Hermitian picture. Thus, the transmission function $\mathcal{T}_{ij}(\omega)$ is specified as

$$\mathcal{T}_{ij}(\omega) = \sum_{n,m} \frac{\langle\psi_m|\hat{\Gamma}_i|\psi_n\rangle\langle\phi_n|\hat{\Gamma}_j|\phi_m\rangle}{(\omega - E_{n,\psi})(\omega - E_{m,\phi})\langle\phi_n|\psi_n\rangle\langle\psi_m|\phi_m\rangle}. \tag{9}$$

This formula describes the transmission between the two terminals by doubly summing over all eigenstates, which includes interference terms ($n \neq m$). This is one main point in this study. The key observation is that the transmission function depends not only on the individual eigenvalues $E_{n,\psi}$ and $E_{m,\phi}$, but also on the overlap terms $\langle\phi_n|\psi_n\rangle$ and $\langle\psi_m|\phi_m\rangle$, which measure how strongly the eigenstates of the system are coupled with each other. As

the system approaches an EP, the eigenvalues of $\hat{H}_{\rm eff}$ will become degenerate, and the corresponding eigenvectors coalesce, which may yield additional efficient transferring modes. This behavior is a hallmark of the EP and signals a profound change in the system's transport properties.

Transport signature of non-Hermiticity. We consider a quantum thermoelectric device comprising three coupled quantum dots connected to two external electrodes. This typical setup is well-suited for exploring the interplay between chiral transport, non-Hermitian physics, and thermodynamic properties at the quantum scale. The quantum system is described by the Hamiltonian $\hat{H} = \hat{H}_{\rm QD} + \hat{H}_{\rm lead} + \hat{H}_{\rm I}$,[56,57] where $\hat{H}_{\rm QD}$ is given by Eq. (2), the electrode leads are described as $\hat{H}_{\rm lead} = \sum_{i=\rm l,\,r}\sum_k \varepsilon_{ik}\hat{c}^\dagger_{ik}\hat{c}_{ik}$, and the dot-lead interactions denote $\hat{H}_{\rm I} = \sum_{i,\,k} V_{ik}\hat{c}^\dagger_i\hat{c}_{ik} +$ H.c.. Here, $\hat{c}^\dagger_{ik}$ and $\hat{c}_{ik}$ create and annihilate an electron in the i-th electrode with the energy ε_{ki}. The quantum dissipation is characterized as the dissipation strength $\gamma_j = 2\pi\sum_k |V_{jk}|^2\delta(\omega-\varepsilon_{jk})$.

This simplified model, devoid of Coulomb interactions, focuses on the non-interacting regime, allowing for an analytical understanding of the role of EPs and chiral transport in quantum thermodynamics. In particular, the dynamics governed by this Hamiltonian can explain the emergence of robust chiral currents and the influence of EPs on transport efficiency. The coupling to the reservoirs sets the stage for exploring thermoelectric effects, energy harvesting, and dissipation mechanisms at the nanoscale, underscoring the relevance of non-Hermitian quantum thermodynamics.

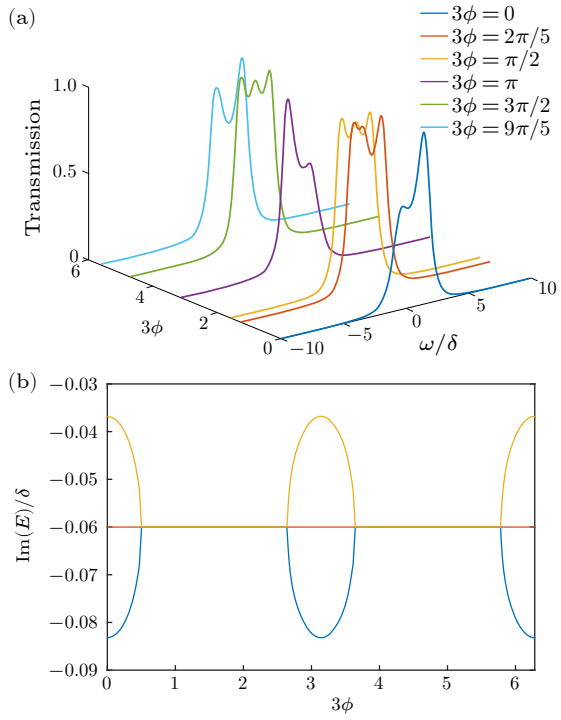

Fig. 5. (a) The transmission function $\mathcal{T}(\omega) = \mathcal{T}_{12}(\omega) + \mathcal{T}_{13}(\omega)$ as a function of ω and (b) the imaginary parts of eigenvalues in the three-terminal triple quantum dots system for different ϕ (in units of $2\pi/3$). The other parameters are given by $\gamma_1 = 5/2\delta$, $\gamma_2 = 1/2\delta$, $\gamma_3 = 3/2\delta$, and $\varepsilon_1 = \varepsilon_2 = \varepsilon_3 = 0$.

Based on the Green function operator at Eq. (7) we construct the effective Hamiltonian of chiral triple quantum dots

$$\hat{H}_{\rm eff} = \hat{H}_{\rm QD} + {\rm i}\hat{\Gamma}/2, \tag{10}$$

which plays a central role in determining the quantum transport of the triple-QD system, as it encapsulates both the coherent dynamics and the dissipative effects. To obtain the analogous Hamiltonian at Eq. (1) with effective gain-loss processes, we set the asymmetric condition of dissipation strengths $\gamma_1 \neq \gamma_2$ and $\gamma_3 = (\gamma_1+\gamma_2)/2$. Therefore, by introducing $\hat{H}'_{\rm eff} = \hat{H}_{\rm eff} - {\rm i}(\gamma_1+\gamma_2)\hat{I}/4$, it is straightforward to find $H'_{\rm eff}$ is equivalent with the gain-loss effective Hamiltonian at Eq. (1) with the gain (loss) strength $(\gamma_1-\gamma_2)/4$. Hence, the real parts of eigenvalues of $\hat{H}_{\rm eff}$ are identical with the one at Eq. (1). In the following, the dissipation strengths are specified as $\gamma_1 = \gamma$, $\gamma_2 = \gamma/5$, and $\gamma_3 = 3\gamma/5$.

We investigate the possible signature of EPs from peaks of the transmission function $\mathcal{T}(\omega) = \mathcal{T}_{12}(\omega)+\mathcal{T}_{13}(\omega)$ as a function of energy ω for different values of the chiral phase ϕ (in the period of $2\pi/3$) with weak dissipation strength, e.g., $\gamma/\delta = 1$ in Fig. 5(a). When the chiral phase is zero, the transmission function shows a single main peak in the $\mathcal{PT}$ symmetry-breaking regime, as exhibited in Fig. 5(b). The position of the main peak can be determined via ${\rm Re}(E_1)$, which is in absence of degeneracy. The magnitude is quantified as $\mathcal{G}_{1,1}[{\rm Re}(E_1)]$, with

$$\mathcal{G}_{n,m}(\omega) = \sum_{j=2,3}\frac{\langle\psi_m|\hat{\Gamma}_1|\psi_n\rangle\langle\phi_n|\hat{\Gamma}_j|\phi_m\rangle}{(\omega-E_{n,\,\psi})(\omega-E_{m,\,\phi})\langle\phi_n|\psi_n\rangle\langle\psi_m|\phi_m\rangle}. \tag{11}$$

We numerically find $\mathcal{G}_{1,1}[{\rm Re}(E_1)] \approx 1$, which demonstrates that the non-Hermitian eigenstate $|\psi_1\rangle$ of $\hat{H}_{\rm eff}$ is the efficient mode to transfer energy and matter. As the phase approaches $\phi^{\rm c}_{1,+}$, i.e., the position of EP2, the structure of two main peaks appears, corresponding to two distinct values of ${\rm Re}(E_q)$ $(q = 1, 2)$ [${\rm Re}(E_2)$ has two-fold degeneracies], with the magnitude of the new peak quantified as $\{\sum_{n,\,m=2,\,3}\mathcal{G}_{n,\,m}[{\rm Re}(E_2)]\}$ and the other one $\mathcal{G}_{1,1}[{\rm Re}(E_1)]$. Meanwhile, the maximal magnitudes of both peaks are both nearly 1, which show two efficient transferring modes in the non-Hermitian picture. Suppose one continues to tune up ϕ to enter the $\mathcal{PT}$-symmetry regime, three apparent peaks occur, mainly due to three distinct real parts of eigenvalues and finite identical imaginary parts. The magnitudes of peaks are characterized as $\mathcal{G}_{q,\,q}[{\rm Re}(E_q)]$ $(q = 1, 2, 3)$. If the ϕ gets close to $\phi^{\rm c}_{1,-}$, i.e., another EP2, two real parts of eigenvalues become degenerate again. Hence, the structure of the transmission function is reduced to two-peak form. Accordingly, the effective modes are reduced to two. When ϕ is in the regime $(\phi^{\rm c}_{1,\,-}, \pi/3)$, the transmission function shows one main peak dominated by the eigenvalue without the degeneracy of real parts. While the eigenstates and eigenvalues of $\hat{H}_{\rm eff}$ show a mirror feature at the point $\pi/3$.

If we enlarge the dissipation strengths, e.g., $\gamma/\delta = 5\sqrt{3}/2$, only one peak is exhibited, mainly due to the dramatic broadening of the eigenvalues with large imaginary

parts compared to the real ones. Then the peak detection via the transmission function becomes inefficient. Therefore, we conclude that with weak quantum dissipations, the transmission function behaves as (i) three main peaks in most of $\mathcal{PT}$-symmetry regimes, (ii) two main peaks around EPs, and (iii) single main peak in most of $\mathcal{PT}$-symmetry breaking regimes.

We note that the above investigation of the EP feature and transmission function is both based on the Hilbert space of coupled quantum dots. This is distinct from the bosonic counterpart, of which the EP signature is calculated from the framework of boson modes, rather than the Hilbert space. Hence, the calculation of transmission $\mathcal{T}(\omega)$ generally does not correspond to the EP behavior.

Conclusion. In this work, we investigate the properties of a non-Hermitian triple-quantum-dot system, with a particular focus on the interplay between the chiral field, tunneling interactions, and incoherent gain and loss processes. By tuning the chiral phase and tunneling amplitude, we demonstrate the emergence of second- and third-order EPs, which govern the system's spectral singularities and chiral transport.

We delve into the interplay between $\mathcal{PT}$ symmetry and non-Hermitian effects. The evolution of the chiral current shows significant variations across three distinct scenarios, depending on the ratio γ/δ. Additionally, we connect the non-Hermitian nature of the system to the peak features observed in the transmission function, which serves as a tool for detecting these exotic behaviors. A general framework for constructing the transmission function within the non-Hermitian picture is introduced, revealing three main types of peaks.

These findings contribute to the expanding field of non-Hermitian transport, offering valuable insights for the design and optimization of chiral and non-Hermitian quantum devices. Our results also lay the groundwork for future research in the engineering of non-Hermitian quantum systems, with potential applications in enhancing thermoelectric performance, quantum sensing, and other advanced quantum technologies. Finally, our study does not involve the roles of electron-photon and electron-electron interactions. The generalization of the non-Hermitian physics in mesoscopic transport through cavity-coupled double quantum-dots[58] should be intriguing in future studies.

Acknowledgements. This work was supported by the National Key R&D Program of China (Grant No. 2022YFA1404400), the National Natural Science Foundation of China (Grant No. 12125504 and 12305050), Zhejiang Provincial Natural Science Foundation of China (Grant No. LZ25A050001), the Hundred Talents Program of the Chinese Academy of Sciences, and the Natural Science Foundation of Jiangsu Higher Education Institutions of China (Grant No. 23KJB140017).

References

[1] Ashida Y, Gong Z, and Ueda M 2020 *Adv. Phys.* **69** 249
[2] Bender C M and Hook D W 2024 *Rev. Mod. Phys.* **96** 045002
[3] Pan L, Chen X, Chen Y, and Zhai H 2020 *Nat. Phys.* **16** 767
[4] Kang M, Chen J, and Chong Y D 2016 *Phys. Rev. A* **94** 033834
[5] Wang A X, Meng Z Q, and Chen C Q 2023 *Sci. Adv.* **9** eadf7299
[6] Zhu W, Deng W, Liu Y, Lu J, Wang H X, Lin Z K, Huang X, Jiang J H, and Liu Z 2023 *Rep. Prog. Phys.* **86** 106501
[7] Rüter C E, Makris K G, El-Ganainy R, Christodoulides D N, Segev M, and Kip D 2010 *Nat. Phys.* **6** 192
[8] Feng L, El-Ganainy R, and Ge L 2017 *Nat. Photon.* **11** 752
[9] Miri M A and Alù A 2019 *Science* **363** eaar7709
[10] Wang C, Fu Z, Mao W, Qie J, Stone A D, and Yang L 2023 *Adv. Opt. Photon.* **15** 442
[11] Shi C Z, Dubois M, Chen Y, Cheng L, Ramezani H, Wang Y, and Zhang X 2016 *Nat. Comm.* **7** 11110
[12] Wang X, Fang X S, Mao D X, Jing Y, and Li Y 2019 *Phys. Rev. Lett.* **123** 214302
[13] Gu Z, Gao H, Cao P C, Liu T, Zhu X F, and Zhu J 2021 *Phys. Rev. Applied* **16** 057001
[14] El-Ganainy R, Makris K G, Khajavikhan M, Musslimani Z H, Rotter S, and Christodoulides D N 2018 *Nat. Phys.* **14** 11
[15] Bender C M and Boettcher S 1998 *Phys. Rev. Lett.* **80** 5243
[16] Hodaei H, Hassan A U, Wittek S, Garcia-Gracia H, El-Ganainy R, Christodoulides D N, and Khajavikhan M 2017 *Nature* **548** 187
[17] Chen W J, Özdemir Ş K, Zhao G M, Wiersig J, and Yang L 2017 *Nature* **548** 192
[18] Wiersig J 2020 *Photon. Res.* **8** 1457
[19] Franke J, Muleady S R, Kaubruegger R, Kranzl F, Blatt R, Rey A M, Joshi M K, and Roos C F 2023 *Nature* **621** 740
[20] Zhang J W, Zhang J Q, Ding G Y, Li J C, Bu J T, Wang B, Yan L L, Su S L, Chen L, Nori F, Özdemir Ş K, Zhou F, Jing H, and Feng M 2022 *Nat. Commun.* **13** 6225
[21] Bu J T, Zhang J Q, Ding G Y, Li J C, Zhang J W, Wang B, Ding W Q, Yuan W F, Chen L, Özdemir Ş K, Zhou F, Jing H, and Feng M 2023 *Phys. Rev. Lett.* **130** 110402
[22] Okuma N, Kawabata K, Shiozaki K, and Sato M 2020 *Phys. Rev. Lett.* **124** 086801
[23] Li L H, Lee C H, Mu S, and Gong J B 2020 *Nat. Comm.* **11** 5491
[24] Liang Q, Xie D, Dong Z, Li H, Li H, Gadway B, Yi W, and Yan B 2022 *Phys. Rev. Lett.* **129** 070401
[25] Zhang X, Zhang T, Lu M H, and Chen Y F 2022 *Adv. Phys. X* **7** 2109431
[26] Li Z, Wang L W, Wang X, Lin Z K, Ma G, and Jiang J H 2024 *Nat. Commun.* **15** 6544
[27] Sunada S 2017 *Phys. Rev. A* **96** 033842
[28] Lai Y H, Lu Y K, Suh M G, Yuan Z Q, and Vahala K 2019 *Nature* **576** 65
[29] Bergholtz E J, Budich J C, and Kunst F K 2021 *Rev. Mod. Phys.* **93** 015005
[30] Ding K, Fang C, and Ma G 2022 *Nat. Rev. Phys.* **4** 745
[31] Okuma N and Saito M 2023 *Ann. Rev. Cond. Matt. Phys.* **14** 83
[32] Budich J C and Bergholtz E J 2020 *Phys. Rev. Lett.* **125** 180403
[33] Han P R, Ning W, Huang X J, Zheng R H, Yang S B, Wu F, Yang Z B, Su Q P, Yang C P, and Zheng S B 2024 *Nat. Comm.* **15** 10293
[34] Khandelwal S, Brunner N, and Haack G 2021 *PRX Quantum* **2** 040346
[35] Abo S, Tulewicz P, Bartkiewicz K, Özdemir Ş K, and Miranowicz A 2024 *New J. Phys.* **26** 123032

[36] Zhou Y L, Yu X D, Wu C W, Li X Q, Zhang J, Li W B, and Chen P X 2023 *Phys. Rev. Research* **5** 043036

[37] Lodahl P, Mahmoodian S, Stobbe S, Rauschenbeutel A, Schneeweiss P, Volz J, Pichler H, and Zoller P 2017 *Nature* **541** 473

[38] Downing C A, Zueco D, and Martín-Moreno L 2020 *ACS Photonics* **7** 3401

[39] Katsnelson M I, Novoselov K S, and Geim A K 2006 *Nat. Phys.* **2** 620

[40] Raghu S and Haldane F D M 2008 *Phys. Rev. A* **78** 033834

[41] Lu Z G, Wu Y, and Lü X Y 2025 *Phys. Rev. Lett.* **134** 013602

[42] Ryu S, López R, Serra L, and Sánchez D 2022 *Nat. Comm.* **13** 2512

[43] Bu J T, Zhang J Q, Ding G Y, Li J C, Zhang J W, Wang B, Ding W Q, Yuan W F, Chen L, Zhong Q, Keçebaş A, Özdemir Ş K, Zhou F, Jing H, and Feng M 2024 *Light: Science, and Applications* **13** 143

[44] Xu G Q, Zhou X, Li Y, Cao Q T, Chen W J, Xiao Y F, Yang L, and Qiu C W 2023 *Phys. Rev. Lett.* **130** 266303

[45] del Pino J, Slim J J, and Verhagen E 2022 *Nature* **606** 82

[46] Shu X Q, Zhong Q, Hong K, You O B, Wang J, Hu G W, Alù A, Zhang S, Christodoulides D N, and Chen L 2024 *Light: Science, and Applications* **13** 65

[47] Ye R, He Y Y, Li G Z, Wang L J, Wu X X, Qiao X, Zheng Y L, Jin L, Wang D W, Yuan L Q, and Chen X F 2025 *Light: Science, and Applications* **14** 39

[48] Liu Y Y, Stehlik J, Eichler C, Gullans M J, Taylor J M, and Petta J R 2015 *Science* **347** 285

[49] Coskun U C, Wei T C, Vishveshwara S, Goldbart P M, and Bezryadin A 2004 *Science* **304** 1132

[50] Engelhardt G and Cao J S 2019 *Phys. Rev. B* **99** 075436

[51] Haug H and Jauho A P 2008 *Quantum Kinetics in Transport, and Optics of Semiconductors* (Springer-Verlag, Berlin, Heidelberg)

[52] Landauer R 1970 *The Philosophical Magazine: A Journal of Theoretical Experimental, and Applied Physics* **21** 863

[53] Datta S 2005 *Quantum Transport: Atom to Transistor* (Cambridge University Press, London)

[54] Chen Y and Zhai H 2018 *Phys. Rev. B* **98** 245130

[55] Shen P X, Lu Z D, Lado J L, and Trif M 2024 *Phys. Rev. Lett.* **133** 086301

[56] Wang R, Wang C, Lu J, and Jiang J H 2022 *Adv. Phys. X* **7** 2082317

[57] Lu J, Liu Y, Wang R, Wang C, and Jiang J H 2019 *Phys. Rev. B* **100** 115438

[58] Lu J, Wang R, Ren J, Kulkarni M, and Jiang J H 2019 *Phys. Rev. B* **99** 035129